Publishing Excellence Inspiring Progress
ARISTON PUBLICATIONS
Energy & Environment Advances
ISSN: 3066-5728 https://aristonpubs.com/energy-environment-advances https://doi.org/10.69626/eea.2025.0141

RESEARCH ARTICLE

Enhanced Photocatalytic Degradation of Methyl Red Dye Using Hydrothermally Synthesized Cadmium Oxide Nanorods

A. K. Barve [1,*], R. B. Lanjewar [2]

ABSTRACT: This study presents a simple hydrothermal approach for synthesizing cadmium oxide (CdO) nanorods, utilizing cadmium chloride as a precursor with polyethylene glycol and urea serving as stabilizing agents. The structural, morphological, and optical properties of the as-prepared nanorods were systematically investigated through X-ray diffraction (XRD), transmission electron microscopy (TEM), UV–visible spectroscopy, and Fourier-transform infrared (FTIR) spectroscopy. XRD analysis revealed a cubic crystalline phase with an average crystallite size of approximately 65 nm, a finding consistent with TEM observations, which showed spherical nanorods with sizes ranging between 60–70 nm. FTIR spectra confirmed the presence of Cd–O bonds, while UV–visible absorption measurements indicated a notable blue shift and an increased optical band gap of 3.75 eV, attributed to quantum confinement effects. The photocatalytic performance of the CdO nanorods was evaluated through the degradation of methyl red dye under UV irradiation. Results demonstrated efficient dye degradation, particularly at lower concentrations, with the process following pseudo-first-order kinetics. The study underscores the potential of hydrothermally synthesized CdO nanorods as effective photocatalysts for the remediation of dye-contaminated wastewater, offering a sustainable and eco-friendly treatment option.

Keywords: Hydrothermal synthesis, Cadmium oxide nanorods, Photocatalysis, Methyl red degradation, Quantum confinement, Wastewater treatment.

Received: 13 February 2025; Revised: 03 May 2025; Accepted: 09 June 2025; Published Online: 26 July 2025

1. INTRODUCTION

The escalating contamination of water resources by industrial effluents stands as one of the most pressing environmental challenges of our time [1]. Among the diverse pollutants, synthetic dyes discharged from textile, paper, and printing industries are particularly problematic due to their complex aromatic structures, which render them highly resistant to natural degradation processes [2-4]. These compounds not only impart undesirable colour to water bodies, reducing light penetration and disrupting aquatic ecosystems, but many are also toxic, carcinogenic, and pose significant risks to human health upon exposure [5, 6]. Methyl red, a common anionic azo dye, exemplifies this issue; its widespread use and persistent nature necessitate the development of effective remediation strategies [7].

Conventional wastewater treatment methods, including adsorption and biological processes, often prove inadequate for complete dye mineralisation, merely transferring the pollutant from one phase to another or generating secondary sludge [8]. In this context, advanced oxidation processes (AOPs) have emerged as powerful alternatives, with semiconductor-mediated photocatalysis being especially promising. This technology utilises light energy to generate highly reactive oxidative species on a catalyst surface, capable of mineralising complex organic molecules into harmless inorganic compounds like CO_2 and H_2O, offering a

[1] Ajeenkya D. Y. Patil School of Engineering, Savitribai Phule Pune University, Lohegoan, Pune-411081, India
[2] Dharampeth M.P. Deo Memorial Science College, North Ambazari Road, Nagpur-440033, Maharastra, India

* Author to whom correspondence should be addressed: drashwinibokade@gmail.com (A. K. Barve)

© Ariston Publications 2025. All rights reserved.

potentially green and sustainable solution for water purification [9-11].

Cadmium oxide (CdO), an n-type semiconductor from the II-VI group, has garnered substantial interest for its remarkable suite of physical and chemical properties, which underpin its utility in a range of technological applications. Its intrinsic characteristics, including high electrical conductivity even in undoped states, attributed to native defects such as oxygen vacancies and cadmium interstitials, make it valuable for transparent conducting electrodes, gas sensors, phototransistors, and photovoltaic devices [12, 13]. Optically, CdO possesses a direct band gap of approximately 2.2 eV and an indirect gap of 1.36 eV in its bulk form, allowing it to interact with visible light [4, 14]. Beyond these optoelectronic applications, the potential of CdO as a photocatalytic material has been progressively uncovered. The fundamental principle involves the irradiation of the semiconductor with photons of energy equal to or greater than its band gap, which excites electrons from the valence band to the conduction band, creating electron-hole pairs. These charge carriers can migrate to the surface and participate in redox reactions with adsorbed species, such as water and oxygen, to produce hydroxyl radicals (•OH) and superoxide anions ($O_2^{\bullet-}$), which are potent oxidising agents for organic pollutants [5-7, 15-19]. Previous studies have indeed demonstrated the capability of CdO to degrade various dyes and environmental contaminants, establishing its photocatalytic credentials [6, 7, 20-23].

The synthesis pathway plays a critical role in defining the morphological, structural, and ultimately, the functional properties of semiconductor nanomaterials. Various techniques have been employed to fabricate CdO nanostructures, including sol-gel processes, spray pyrolysis, chemical vapour deposition, and chemical bath deposition [3, 4]. Each method imparts distinct characteristics concerning particle size, crystallinity, surface area, and defect chemistry. Among these, the hydrothermal method offers distinct advantages for crafting nanorods with controlled features. It is a solution-based technique conducted in a sealed autoclave at elevated temperature and pressure, which promotes high crystallinity, narrow size distribution, and often unique morphologies without the need for post-annealing at high temperatures. The novelty of the present work lies in the employment of a facile, one-pot hydrothermal protocol using cadmium chloride, polyethylene glycol, and urea to produce CdO nanorods. This specific combination of precursors and stabilizer is designed to yield particles with a high surface area and controlled nano-dimensions, which are anticipated to enhance photocatalytic performance through quantum confinement effects and increased active sites. Furthermore, a systematic investigation linking the synthesized nanomaterial's intrinsic properties, such as its enlarged band gap and nanostructure, to its efficiency in degrading methyl red under UV illumination, with a particular focus on the kinetic implications of varying initial dye concentrations, constitutes a significant contribution to the rational design of CdO-based photocatalysts.

The photocatalytic degradation process is influenced by a complex interplay of factors, including the catalyst's surface properties, the optical absorption characteristics, and the reaction environment. Azo dyes like methyl red, characterised by the presence of -N=N- bonds and sulphonate groups, present a challenging target for degradation due to their stability [10, 11]. The efficiency of their breakdown via photocatalysis depends on the catalyst's ability to generate and utilise photogenerated charge carriers before they recombine. Therefore, comprehensive characterisation of the synthesised material is paramount. In this study, the structural phase and crystallite size of the hydrothermally produced CdO nanorods were determined using X-ray diffraction (XRD). Morphological analysis and particle size confirmation were conducted via transmission electron microscopy (TEM). The optical properties and band gap energy were elucidated through UV-visible spectroscopy, while Fourier-transform infrared (FTIR) spectroscopy was employed to confirm chemical bonding and surface characteristics. Subsequently, the photocatalytic prowess of the nanorods was evaluated by monitoring the degradation kinetics of methyl red dye in aqueous solutions under UV light irradiation. This work aims to provide a coherent narrative from synthesis and characterisation to functional application, underscoring the potential of hydrothermally engineered CdO nanorods as effective and sustainable agents for the photocatalytic remediation of dye-laden wastewater.

2. EXPERIMENTAL DETAILS

2.1. Materials

All chemicals employed in this synthesis were of analytical reagent grade and used without further purification. Cadmium chloride ($CdCl_2$), ethylene glycol ($C_2H_6O_2$), and urea (CH_4N_2O) were procured from S.D. Fine Chemicals Ltd. The target pollutant, Methyl Red dye ($C_{15}H_{15}N_3O_2$), was an AR-grade product obtained from Merck. All aqueous solutions were prepared using deionized water with a resistivity of 18.2 MΩ·cm.

2.2. Synthesis of CdO Nanorods

Cadmium oxide nanorods were synthesized via a modified hydrothermal route. In a typical procedure, 30 mL of ethylene glycol, acting as a stabilizer and reaction medium, was mixed with 50 mL of a 1 M aqueous solution of cadmium chloride. This mixture was magnetically stirred vigorously for 30 minutes at ambient temperature to ensure homogeneity. Subsequently, 50 mL of a 1 M urea solution was introduced dropwise into the stirring mixture, which immediately resulted in the formation of a milky white suspension, indicating the onset of precursor hydrolysis and condensation. The final reaction mixture was transferred into a 150 mL Teflon-lined stainless-steel autoclave, which was sealed and maintained at 180°C for a duration of 1 hour in a hot-air oven. The elevated temperature and autogenous pressure within the

 © Ariston Publications 2025. All rights reserved

autoclave facilitated the crystallization of the product. After the reaction, the autoclave was allowed to cool naturally to room temperature. The resulting white precipitate was collected by centrifugation, then subjected to a thorough washing sequence with deionized water and absolute ethanol three times each to remove any ionic residues and organic by-products. The purified product was finally dried in a hot-air oven at 150°C for 5 hours to yield a fine, free-flowing powder of CdO nanorods, which was stored for subsequent characterization and photocatalytic testing.

2.3. Characterization Techniques

The crystalline phase and structural parameters of the synthesized powder were determined using a Bruker D8 Advance X-ray diffractometer operated with Cu Kα radiation (λ = 1.5406 Å) at 40 kV and 40 mA. Data was collected in the 2θ range of 10° to 80°. The morphological features, particle size distribution, and selected area electron diffraction (SAED) patterns were investigated using a JEOL JEM-2100 transmission electron microscope operating at an accelerating voltage of 200 kV. For TEM analysis, a sample was prepared by dispersing the powder in ethanol via ultrasonication and depositing a drop onto a carbon-coated copper grid. Fourier-transform infrared (FTIR) spectra were recorded in the range of 400–4000 cm^{-1} on a Shimadzu IRSpirit spectrometer using the KBr pellet method to identify functional groups and confirm metal-oxygen bonding. The optical absorption properties were studied using a Shimadzu UV-1800 double-beam spectrophotometer in the wavelength range of 200–800 nm, with the sample dispersed in deionized water. The photocatalytic activity was also monitored using this spectrophotometer by measuring the characteristic absorption peak of Methyl Red dye at λ_{max} = 430 nm.

3. RESULTS AND DISCUSSION

3.1. Structural and Phase Analysis: XRD

The crystalline structure and phase purity of the as-synthesized product were ascertained using X-ray diffraction analysis. The obtained XRD pattern is displayed in Figure 1. All the discernible diffraction peaks are sharp and well-defined, confirming the highly crystalline nature of the material. These peaks can be systematically indexed to the (012), (110), (111), (200), and (220) lattice planes of the cubic crystal structure of cadmium oxide (JCPDS card no. 65-2908). The absence of any extraneous peaks attributable to impurities or precursor residues indicates the successful synthesis of a pure CdO phase under the employed hydrothermal conditions. The lattice parameter calculated from these reflections is approximately 2.734 Å, which is in good agreement with standard reported values for cubic CdO. The average crystallite size was estimated from the most intense (111) peak using the Debye-Scherrer formula, $D = (0.94\lambda)/(\beta \cos \theta)$, where λ is the X-ray wavelength, β is the full width at half maximum (FWHM) in radians, and θ is the Bragg diffraction angle. The calculated average crystallite size was found to be approximately 65 nm. This value provides a primary estimate of the domain size within the nanorods and serves as a basis for comparison with direct microscopic observation.

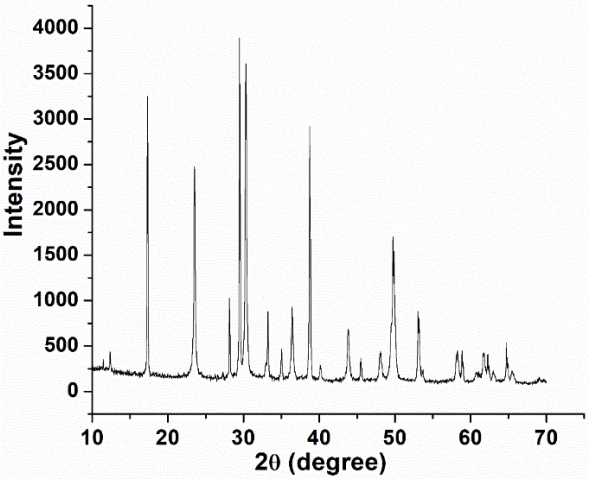


Fig. 1. XRD pattern of hydrothermally synthesized CdO nanorods, confirming a cubic crystalline phase.

3.2. Functional Group Analysis: FTIR Spectroscopy

Fourier-transform infrared spectroscopy was employed to investigate the surface chemistry and confirm the formation of Cd-O bonds. The FTIR spectrum of the synthesized powder is presented in Figure 2. In the high-frequency region, a broad and complex band spanning from approximately 3199 cm^{-1} to 3518 cm^{-1} is observed. This envelope can be deconvoluted into contributions from the O-H stretching vibrations of adsorbed water molecules and the N-H symmetric and asymmetric stretching modes from residual urea or its decomposition products. The presence of these bands indicates some surface hydration and the organic capping role played by the precursors during synthesis. More critically, in the lower frequency region, a distinct and sharp peak is evident at 723 cm^{-1}. This absorption is a characteristic signature of the stretching vibration of the metal-oxygen bond, specifically the Cd-O bond, confirming the formation of cadmium oxide [12]. Furthermore, a broad absorption band centered around 420 cm^{-1}, which is another fingerprint region for Cd-O lattice vibrations, further corroborates the successful synthesis of the target oxide. The spectrum confirms that despite the organic precursors used, the core product is CdO, with surface-adsorbed species that are typical for Nanorods synthesized in aqueous media.

3.3. Morphological and Crystallographic Analysis

The morphology, size, and crystalline nature of the nanorods were directly visualized using transmission electron microscopy.

© Ariston Publications 2025. All rights reserved.

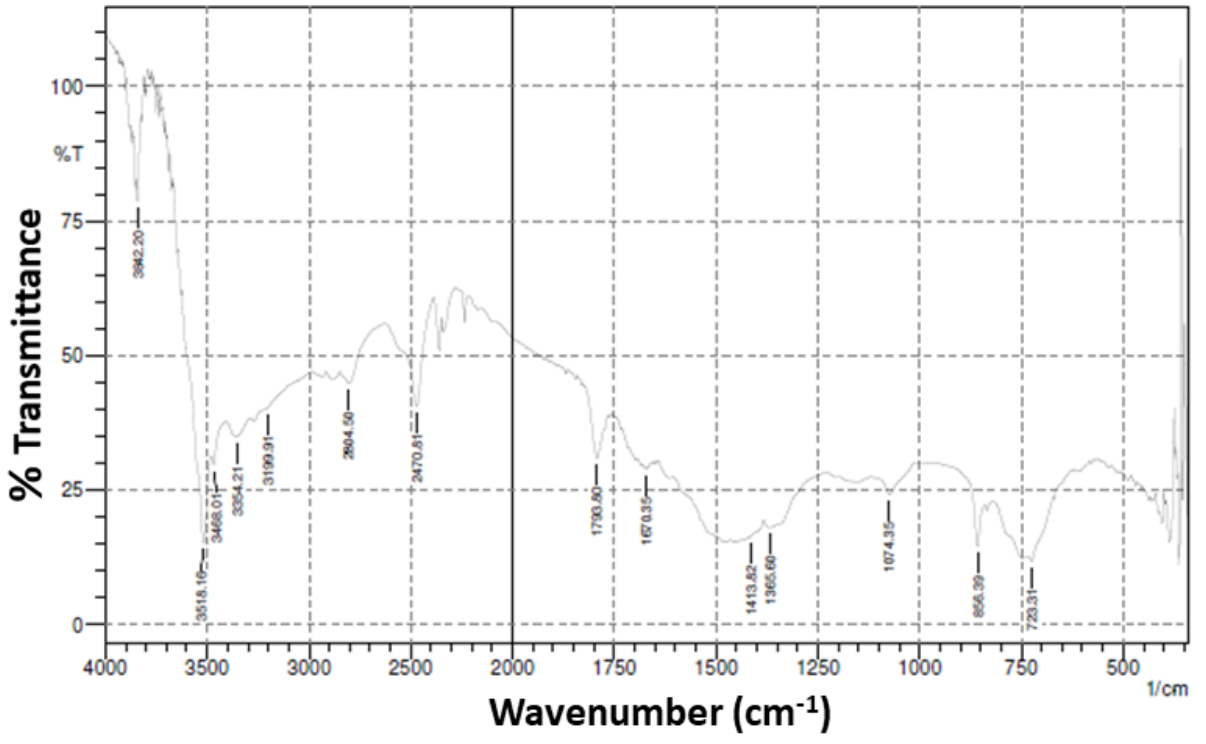


Fig. 2. FTIR spectra of the CdO Nanorods, showing characteristic Cd-O bonding and surface functional groups.

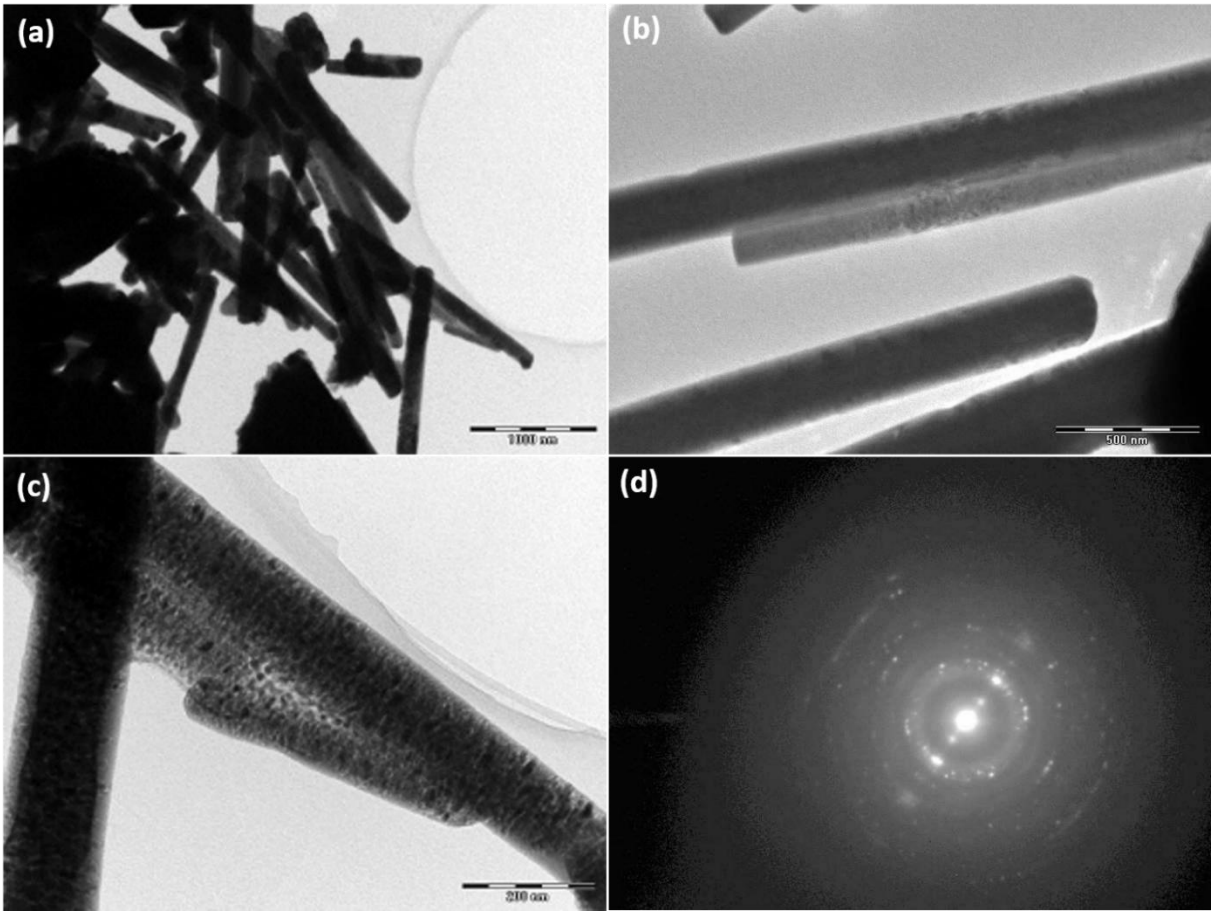


Fig. 3. (a-c) TEM micrographs, and (d) corresponding SAED pattern of CdO Nanorods, revealing spherical morphology and polycrystalline nature.

 © Ariston Publications 2025. All rights reserved

Representative TEM images are shown in Figure 3 (a-c). The micrographs reveal that the primary particles are predominantly quasi-spherical in shape, with a size distribution ranging between 60 and 70 nm. This observation aligns remarkably well with the crystallite size estimated from XRD line broadening, suggesting that the nanorods are largely single-crystalline. Interestingly, the images also show that the nanorods extending up to several hundred nanometers in length. Figure 3 (d) shows the corresponding selected area electron diffraction (SAED) pattern. The pattern consists of a series of concentric, bright rings composed of discrete spots. These rings can be indexed to the (111), (200), (220), and (311) planes of the cubic CdO structure, which is consistent with the XRD results. The spotted nature of the rings confirms the high crystallinity of the individual nanorods, while the ring pattern itself confirms the polycrystalline nature of the sampled area.

3.4. Optical Properties and Band Gap Estimation

The optical absorption properties of the CdO Nanorods were studied using UV-Vis spectroscopy, and the absorption spectrum is shown in **Figure 4**. A strong and broad absorption onset is observed with a maximum around 330 nm. This represents a significant blue shift compared to the absorption edge of bulk CdO, which typically lies in the visible region (around 550-600 nm corresponding to its ~2.2 eV band gap). This shift is a direct manifestation of the quantum confinement effect. As the particle size decreases to the nanoscale, the charge carriers become spatially confined, leading to a widening of the effective band gap.

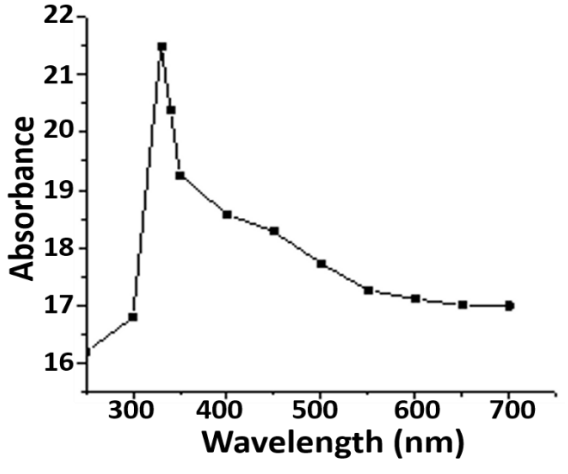


Fig. 4. UV-Visible absorption spectrum of CdO Nanorods dispersed in water, indicating a strong blue shift and widened band gap.

The optical band gap (E_g) was determined from the Tauc plot, derived from the absorption data by plotting $(\alpha h\nu)^2$ versus photon energy ($h\nu$) for a direct band gap semiconductor. The linear portion of this plot was extrapolated to the energy axis to obtain the direct band gap value. The calculated optical band gap for the hydrothermally synthesized CdO Nanorods was found to be 3.75 eV. This substantial increase from the bulk value of 2.2 eV is a clear indicator of strong quantum confinement, confirming that the synthesized particles are in the regime where their electronic properties are size-dependent.

3.5. Photocatalytic Performance and Degradation Kinetics

The photocatalytic activity of the synthesized CdO Nanorods was evaluated by monitoring the degradation of methyl red (MR) dye under UV light irradiation. The progress of the reaction was tracked by measuring the decrease in the characteristic absorption peak of MR at 430 nm. Prior to irradiation, the catalyst-dye suspension was stirred in the dark for 30 minutes to establish adsorption-desorption equilibrium, ensuring that subsequent changes were due solely to photocatalytic action. The temporal evolution of the absorption spectra for a typical dye concentration (e.g., 20 ppm) is conceptually represented in Figure 5(a), showing a steady decrease in absorbance with increasing irradiation time.

The degradation kinetics were analyzed for various initial dye concentrations (10-50 ppm), as shown in Figure 5(b). The plots of $\ln(C_0/C)$ versus irradiation time were found to be linear, indicating that the photocatalytic degradation of methyl red follows pseudo-first-order kinetics, consistent with the Langmuir-Hinshelwood model. The apparent rate constant (k) was derived from the slope of these linear fits. A critical observation is that while the absolute amount of dye degraded increases with higher initial concentration, the efficiency or percentage degradation decreases. This is clearly illustrated in Figure 5(c), which plots percentage degradation against time for different concentrations.

The highest degradation efficiency was achieved at the lowest dye concentration (10 ppm).This concentration-dependent behavior can be explained by considering the surface chemistry of the photocatalytic process. At a fixed catalyst loading and light intensity, the number of active sites and the flux of photogenerated charge carriers (electrons and holes) are constant. As the initial dye concentration increases, more dye molecules compete for adsorption on these limited active sites. Consequently, a higher proportion of the catalyst surface becomes covered, reducing the sites available for the adsorption of water and oxygen molecules, which are crucial for forming the primary oxidizing agents, hydroxyl radicals (•OH) and superoxide anions ($O_2^{\bullet-}$). Furthermore, at very high dye concentrations, the dye molecules themselves can act as internal light filters, shielding the catalyst surface from the incident UV photons, thereby reducing the rate of electron-hole pair generation. This interplay of surface saturation and light screening leads to a reduction in the observed degradation efficiency with increasing pollutant load, a phenomenon widely reported in heterogeneous photocatalysis, including for benchmark catalysts like TiO_2 [14, 15].

© Ariston Publications 2025. All rights reserved.

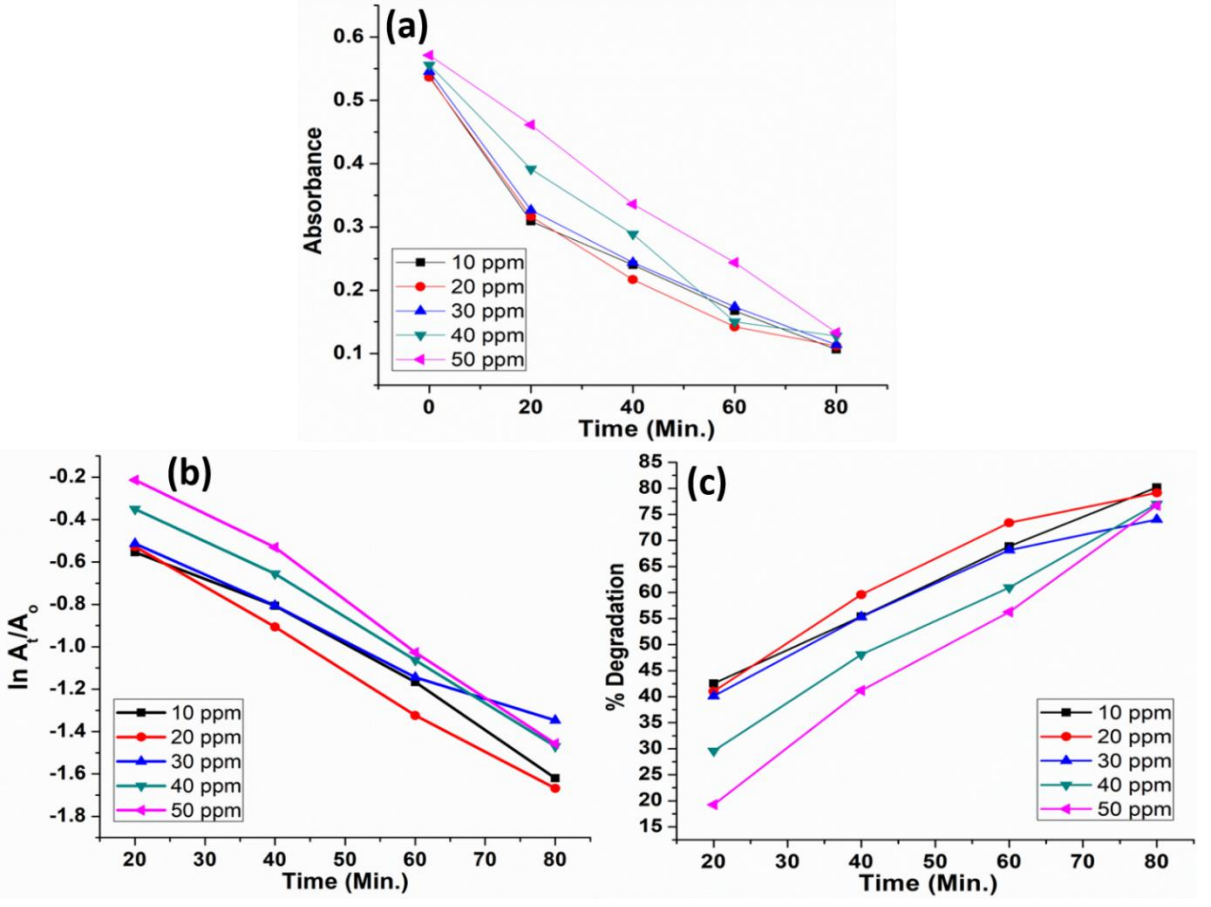


Fig. 5. (a) Temporal decrease in absorbance spectra of Methyl Red dye during photocatalytic degradation; (b) Pseudo-first-order kinetic plots for the photodegradation of Methyl Red at varying initial concentrations, and (c) Comparison of photocatalytic degradation efficiency over time for different initial dye concentrations.

The results confirm that the hydrothermally synthesized CdO Nanorods, with their defined nanostructure and widened band gap, are effective photocatalysts, particularly for treating wastewater with low to moderate organic pollutant concentrations.

4. CONCLUSION

In this work, cadmium oxide Nanorods were successfully synthesized via a facile hydrothermal method and thoroughly characterized to evaluate their structural and optical properties. The Nanorods exhibited a well-defined cubic crystal structure with an average size of ~65 nm, as confirmed by XRD and TEM analyses. Optical studies revealed a significant increase in the band gap to 3.75 eV, a consequence of quantum confinement effects arising from the nanoscale dimensions. The photocatalytic efficiency of the CdO Nanorods was assessed through the degradation of methyl red dye under UV light. It was observed that degradation efficacy was highest at lower dye concentrations, with performance diminishing as concentration increased. This behavior is attributed to the saturation of active sites on the catalyst surface and the limited availability of photogenerated radicals at higher pollutant loadings. The findings highlight the role of surface area and quantum-size effects in enhancing the photocatalytic activity of CdO nanomaterials. Importantly, this study demonstrates that hydrothermally produced CdO Nanorods can serve as effective, low-cost photocatalysts for the decomposition of organic dyes in aqueous environments. While the current results are promising, further research is needed to optimize catalyst loading, explore broader pH ranges, and assess performance under natural sunlight to advance toward practical applications. Overall, the work contributes to the growing body of research on semiconductor-based photocatalysts and supports the potential adoption of CdO Nanorods in sustainable wastewater treatment technologies.

DECLARATIONS

Ethical Approval

We affirm that this manuscript is an original work, has not been previously published, and is not currently under consideration for publication in any other journal or conference proceedings. All authors have reviewed and

 © Ariston Publications 2025. All rights reserved

approved the manuscript, and the order of authorship has been mutually agreed upon.

Funding

Not applicable

Availability of data and material

The datasets generated and/or analyzed during the current study are available from the corresponding author upon reasonable request.

Conflicts of Interest

The authors declare that they have no financial or personal interests that could have influenced the research and findings presented in this paper. The authors alone are responsible for the content and writing of this article.

Authors' contributions

All authors contributed equally to this work.

REFERENCES

[1] Bote, V., Shinde, B., Chavan, R., Jadhav, A., Ghorpade, R., Jamadade, S., Patil, R., Yadav, J., Chougale, A. and More, V. **2025.** Optimizing Precursor Concentration for Enhanced Morphological and Catalytic Performance of ZnO Nanoparticles in Crystal Violet Dye Degradation. ChemSci Advances 2(2), pp. 104-113; https://doi.org/10.69626/csa.2025.0104.

[2] Kaushal, S., Chand, S., Kumar, A., Sharma, N., Sharma, D., Kumar, D. and Kumar, K. **2025.** Biochar Produced from Dead Pine Needles to Produce Biochar/CuO and Biochar/CuO/BaO for Water and Biomedical Remediation. Energy & Environment Advances 2(1), pp. 32-42; https://doi.org/10.69626/eea.2025.0032.

[3] Shweta Kaushal, S., Thakur, M., Thakur, A., Kumar, P., Jaswal, K. and Kumar, K. **2025.** Green Synthesis of Zinc–Doped Copper Oxalate Frameworks for Efficient Photocatalytic Degradation of Methylene Blue. MatSci Express 2(3), pp. 228-236; https://doi.org/10.69626/mse.2025.0228.

[4] Patil, A., Chavan, R., Jadhav, A., Jatratkar, A., Patil, R., Pawar, N. and Chougale, A. **2025.** pH–Controlled Synthesis of Magnetic Fe_3O_4 Nanoparticles for Enhanced Crystal Violet Dye Degradation via Photo–Fenton Process. ChemSci Advances 2(2), pp. 114-124; https://doi.org/10.69626/csa.2025.0114.

[5] Somasundaram, G., Rajan, J., Sangaiya, P. and Dilip, R., **2019**. Hydrothermal synthesis of CdO nanoparticles for photocatalytic and antimicrobial activities. *Results in Materials*, *4*, p.100044.

[6] Gupta, V.K., Fakhri, A., Tahami, S. and Agarwal, S., 2017. Zn doped CdO nanoparticles: structural, morphological, optical, photocatalytic and anti-bacterial properties. *Journal of colloid and interface science*, *504*, pp.164-170.

[7] Patil, V. G. and Mane, D. V. **2025**. Sonochemical Synthesis and Structural–Thermal Characterization of CdO–ZnO Mixed Oxide Nanoparticles: XRD and Williamson–Hall Analysis. *ChemSci Advances* 2(1), pp. 85-94; https://doi.org/10.69626/csa.2025.0085.

[8] Etefa, H.F. and Dejene, F.B., **2025**. Evaluation of physicochemical properties of cadmium oxide (CdO)-incorporated indium–tin oxide (ITO) nanoparticles for photocatalysis. *Journal of Composites Science*, *9*(1), p.43.

[9] Kumar, S., Ojha, A.K. and Walkenfort, B., **2016**. Cadmium oxide nanoparticles grown in situ on reduced graphene oxide for enhanced photocatalytic degradation of methylene blue dye under ultraviolet irradiation. *Journal of Photochemistry and Photobiology B: Biology*, *159*, pp.111-119.

[10] Mulani, S. R., Bimli, S., Bunkar, R., Samatham, M., Choudhary, E., Patil, A., Yadav, S., Yadav, A., Jadhav, H. and Miglani, A. **2024**. Ni-Doped $LaFeO_3$ Microspheres Composed of Nanoparticles for the Photocatalytic Degradation of Organic Dye. *ChemSci Advances* 1(1), pp. 14-20; https://doi.org/10.69626/csa.2024.0014

[11] Prakash, T., Priyanka, R., Siranjeevi, R., Kumar, E.R., Arunadevi, N. and Alharthi, S.S., **2022.** Evaluation of microstructural, optical, vibrational properties and photocatalytic activity of CdO nanostructure. *Ceramics International*, *48*(22), pp.33653-33659.

[12] Sarker, M.A.R. and Ahn, Y.H., **2023.** Strategic insight into enhanced photocatalytic remediation of pharmaceutical contaminants using spherical CdO nanoparticles in visible light region. *Chemosphere*, *311*, p.137040.

[13] Karunakaran, C., Dhanalakshmi, R., Gomathisankar, P. and Manikandan, G., **2010.** Enhanced phenol-photodegradation by particulate semiconductor mixtures: interparticle electron-jump. *Journal of Hazardous Materials*, *176*(1-3), pp.799-806.

[14] Karthik, K., Dhanuskodi, S., Gobinath, C., Prabukumar, S. and Sivaramakrishnan, S., **2017.** Photocatalytic and

© Ariston Publications 2025. All rights reserved.

antibacterial activities of hydrothermally prepared CdO nanoparticles. *Journal of Materials Science: Materials in Electronics*, *28*(15), pp.11420-11429.

[15] Sivakumar, S., Venkatesan, A., Soundhirarajan, P. and Khatiwada, C.P., **2015.** Synthesis, characterizations and anti-bacterial activities of pure and Ag doped CdO nanoparticles by chemical precipitation method. *Spectrochimica Acta Part A: Molecular and Biomolecular Spectroscopy*, *136*, pp.1751-1759.

[16] Robert Xavier, A., Ravichandran, A.T., Ravichandran, K., Mantha, S. and Ravinder, D., **2016.** Sm doping effect on structural, morphological, luminescence and antibacterial activity of CdO nanoparticles. *Journal of Materials Science: Materials in Electronics*, *27*(11), pp.11182-11187.

[17] Karthik, K., Dhanuskodi, S., Gobinath, C., Prabukumar, S. and Sivaramakrishnan, S., **2019.** Multifunctional properties of CdO nanostructures Synthesised through microwave assisted hydrothermal method. *Materials Research Innovations*, *23*(5), pp.310-318.

[18] Sivakumar, S., Venkatesan, A., Soundhirarajan, P. and Khatiwada, C.P., **2015.** Thermal, structural, functional, optical and magnetic studies of pure and Ba doped CdO nanoparticles. *Spectrochimica Acta Part A: Molecular and Biomolecular Spectroscopy*, *151*, pp.760-772.

[19] Gudla, U.R., Suryanarayana, B., Raghavendra, V., Parajuli, D., Murali, N., Dominic, S., Ramakrishna, Y. and Chandramouli, K., **2021.** Structural, optical and luminescence properties of pure, Fe-doped and glucose-capped CdO Semiconductor nanoparticles for their Antibacterial activity. *Journal of Materials Science: Materials in Electronics*, *32*(3), pp.3920-3928.

[20] Negrescu, A.M., Killian, M.S., Raghu, S.N., Schmuki, P., Mazare, A. and Cimpean, A., **2022.** Metal oxide nanoparticles: review of synthesis, characterization and biological effects. *Journal of Functional Biomaterials*, *13*(4), p.274.

[21] Li, J., Ni, Y., Liu, J. and Hong, J., **2009.** Preparation, conversion, and comparison of the photocatalytic property of Cd $(OH)_2$, CdO, CdS and CdSe. *Journal of Physics and Chemistry of Solids*, *70*(9), pp.1285-1289.

[22] Revathi, V. and Karthik, K., **2018.** Microwave assisted CdO–ZnO–MgO nanocomposite and its photocatalytic and antibacterial studies. *Journal of Materials Science: Materials in Electronics*, *29*(21), pp.18519-18530.

[23] Yathisha, R.O., Nayaka, Y.A., Manjunatha, P., Vinay, M.M. and Purushothama, H.T., **2019.** Doping, structural, optical and electrical properties of Ni2+ doped CdO nanoparticles prepared by microwave combustion route. *Microchemical Journal*, *145*, pp.630-641.

 © Ariston Publications 2025. All rights reserved